Original Paper

NEURO-SIGNALS

Neurosignals 2013;21:213–228
DOI: 10.1159/000337350

Received: August 22, 2011
Accepted after revision: February 20, 2012
Published online: August 1, 2012

Modulation of Action Potential Trains in Rabbit Saphenous Nerve Unmyelinated Fibers

Zhi-Ru Zhu[a, c] Yi-Hui Liu[b] Wei-Gang Ji[d] Jian-Hong Duan[a] San-Jue Hu[a]

[a]Institute of Neuroscience, Fourth Military Medical University, and [b]College of Life Sciences, Shaanxi Normal University, Xi'an, [c]Department of Physiology and [d]College of Pharmacy, Third Military Medical University, Chongqing, PR China

Key Words
Single fiber recording · C fiber · Interstimulus interval · Interspike interval · Conduction velocity · 4-Aminopyridine · ZD7288

Abstract
Usually, the main axon is assumed to faithfully conduct action potentials (APs). Recent data have indicated that neural processing can occur along the axonal path. However, the patterns and mechanisms of temporal coding are not clear. In the present study, single fiber recording was used to analyze activity-dependent modulation of AP trains in the main axons of C fibers in the rabbit saphenous nerve. Trains of 5 superthreshold electrical pulses at interstimulus intervals of 20 or 50 ms were applied to the nerve trunk for 200 s. The interspike intervals (ISIs) for these trains were compared to the input interstimulus intervals. Three basic types of C fibers were observed in response to repeated stimuli: first, the ISI between the first and second AP (ISI_{1-2}) of type 1 was longer than the interstimulus interval; second, the ISI_{1-2} of type 2 showed wavelike fluctuations around the interstimulus interval, and third, the ISI_{1-2} of type 3 exhibited shorter intervals for a long period. Furthermore, both 4-aminopyridine-sensitive potassium and hyperpolarization-activated cation currents were involved in the modulation of ISI_{1-2} of train pulses. These data provide new evidence that multiple modes of neural conduction can occur along the main axons of C fibers.

Introduction

Classically, the role of axons has been limited to the simple propagation of action potentials (APs). The pattern of firing is determined by a number of specialized regions that are responsible for signal integration, such as receptors, the axon hillock, and the synapse. Once initiated, APs propagate regeneratively and distribute uniformly over axonal arbors. Therefore, the axon is usually considered as faithfully carrying signals over long distances and working like a relatively simple relay line [1, 2]. However, recent studies on rat and human axons have challenged this classic view by showing that patterns of spike generation can be modulated as the APs travel down the axons [3–7]. Changes in axonal AP propagation during repetitive stimulation depend on the aftereffects of the preceding APs, that is, that immediately after the conduction of one AP, the axon undergoes a series of

KARGER

E-Mail karger@karger.com
www.karger.com/nsg

1424–862X/13/0214–0213$38.00/0

San-Jue Hu and Jian-Hong Duan
Institute of Neuroscience
Fourth Military Medical University
Xi'an, Shaanxi 710032 (PR China)
Tel. +86 29 8477 4590, E-Mail sjhu@fmmu.edu.cn or duanjh200711@gmail.com

changes in oscillatory excitability, and this has been termed the recovery cycle [8]. In addition, the sequence of changes in axonal excitability after AP firing has been analyzed in detail [5, 9–12]. The recovery cycle can last for several hundreds of milliseconds, which gives rise to periods of enhanced and reduced axonal excitability. Concurrent speeding and slowing of conduction can be observed in the same C fiber in response to a train of twin-pulse stimuli [5, 13]. In previous work conducted by our laboratory, the activity-dependent effect on conduction velocity (CV) was influenced by the frequency and time course of the repeated stimulation as well as the period between conditioning and test pulses [14]. These results suggest that the activity-dependent conduction properties possess non-linear characteristics, which may give rise to complex firing behaviors.

Weidner et al. [5] reported that trains of two and four superthreshold electrical stimuli at varying repetition rates could result in temporal dispersion or narrowing of the interspike interval (ISI) of train impulses. It was concluded that at a given degree of neural accommodation, all afferent C-units exhibit a uniform pattern of aftereffects, independent of fiber class [5]. However, in our recent study of AP firing in the saphenous nerve, when electrical stimulation at different frequencies was used to test the effects of activity-dependent changes in CV, a novel fluctuation of ISIs and three distinct types of conduction failure were observed in the propagation course along C fibers [15]. This result strongly suggests that the effects of previous pulse activity (i.e. aftereffects) on ISIs may have a multiple, nonlinear dynamic courses. Thus, we propose that the ISI in saphenous C fibers might be subjected to distinct patterns of aftereffects, which would exhibit various temporal firing patterns.

In order to verify this hypothesis, regular trains containing 5 pulses for a total of 200 trains were used to repetitively stimulate the saphenous nerve, and changes in the properties of the ISIs in the main axon of single C fibers were measured and analyzed. Three types of C fibers were distinguished according to the distinct patterns of ISI changes, especially the ISI_{1-2} (the ISI between the first and second AP). Both 4-aminopyridine (4-AP)-sensitive potassium current ($I_{4\text{-AP}}$) and hyperpolarization-activated cation current (I_h) were involved in the regulation of ISIs. These results confirmed, at least in part, the existence of temporal pattern processing along the main axon of C fibers; we termed this phenomenon conduction coding.

Materials and Methods

Animals and Surgery

Adult rabbits of both sexes, weighing between 1.8 and 2.2 kg, were used under a research protocol approved by the Fourth Military Medical University. Anesthesia was induced with sodium pentobarbital (40 mg/kg i.v.). The procedure for animal surgery has been published in our previous study [15]. As shown in figure 1a, the saphenous nerve of one hind leg was exposed at three sites where skin pools were prepared. One site was used for electrical stimulation (S), one site for single fiber recording (R), and another site was used for drug application (D).

Electrophysiological Recording of Single C Fiber Discharges in vivo

Electrophysiological recordings of single C fibers from saphenous nerve were made as previously described [15]. Briefly, in the stimulation pool, a pair of platinum stimulating electrodes was placed under the nerve trunk and covered with warm (about 37°C) mineral oil. In the middle drug application pool, the nerve trunk was separated about 4–5 cm. After carefully removing the epiperineurium, this part of the saphenous nerve was covered with warm physiological saline with or without drug. In the recording pool, a fine filament was teased from the saphenous nerve and the proximal site was placed on a pair of platinum electrodes (30 μm in diameter) for single C fiber recording (fig. 1a). APs were amplified and recorded on a computer with a signal sample rate of 10 or 100 KHz. The CV of a fiber was determined by dividing the distance between the stimulating and recording electrodes by the AP latency. Fibers with a CV of <2 m/s were classified as C fibers [16, 17].

Electrical Stimulation

After a single fiber had been identified, the whole nerve trunk was stimulated electrically (pulse duration 0.8 ms). In the present experiment, a standard repeated stimulus with an intensity 50% greater than the threshold was applied and 5 pulses for a total of 200 trains were delivered (1 train / s) (fig. 1b). The interstimulus interval of the quintuplet pulses was selected for 20, 30, and 50 ms according to the experimental requirement. After starting the stimulation protocol, we waited for 10 min between two stimulation series to allow recovery from the effects of each stimulus train.

The initial CV (CV_i) was calculated from the distance between the stimulating and recording electrodes divided by the latency of the first AP. This CV_i was compared with the CV of each AP in response to repetitive stimulus pulses at different intervals, and the ratio, as a percentage of CV_i, was called CV slowing.

Parameters Used to Evaluate the Temporal Coding and Conduction Properties of C Fibers

To investigate the temporal coding changes during stimulation, we calculated the ISI between the first and second AP (ISI_{1-2}) in every quintuplet pulse. The other three ISIs (i.e. ISI_{2-3}, ISI_{3-4}, and ISI_{4-5}) were assessed in the same way. The difference between the interstimulus interval and ISI was named ΔISI. The difference between ISI_{1-2} and the interstimulus interval was termed ΔISI_{1-2}. The other three ΔISIs (i.e. ΔISI_{2-3}, ΔISI_{3-4}, and ΔISI_{4-5}) were assessed in an analogous manner. If two consecutive APs had the same CV, their ISIs should exactly match the interstimulus interval, that is, ΔISI = 0. If the ISI was longer than the

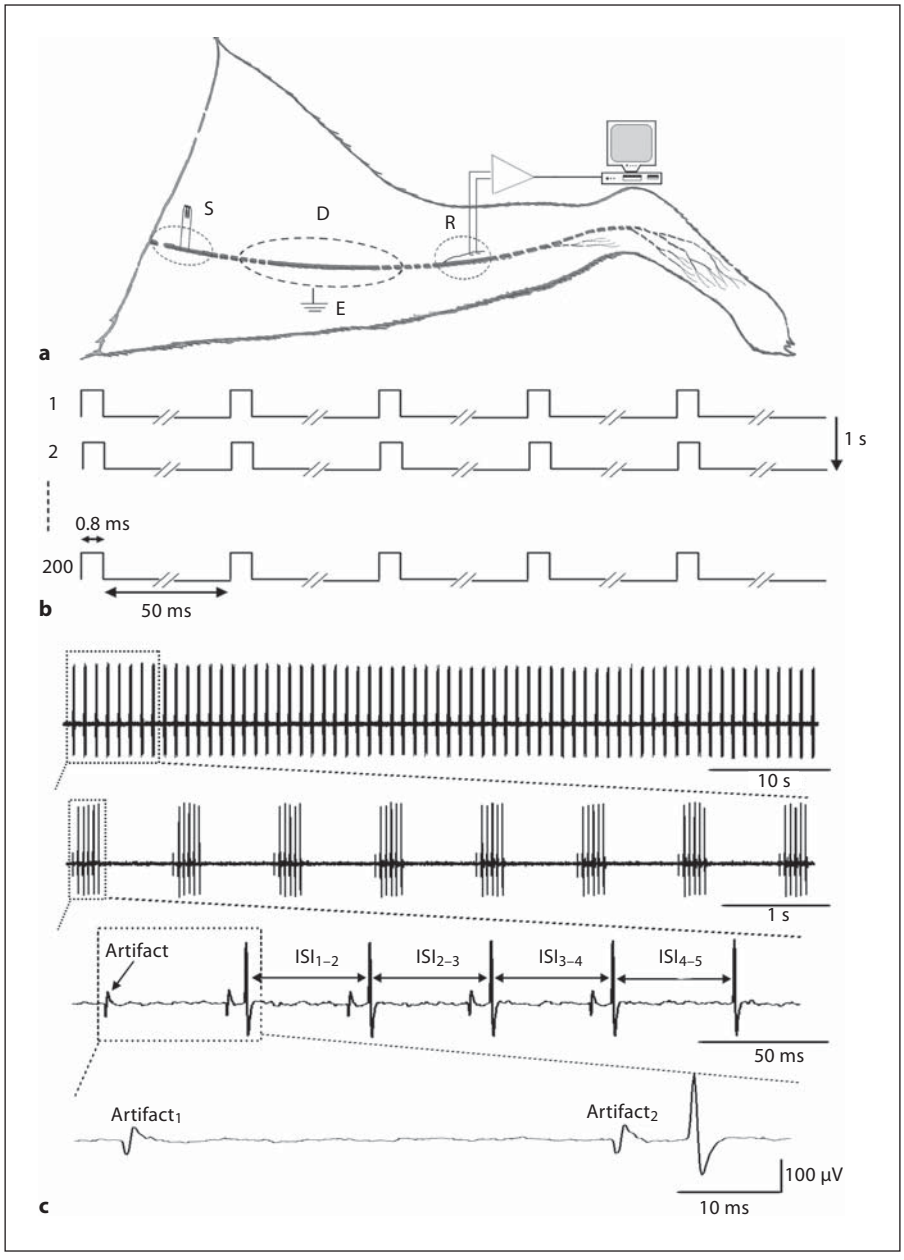

Fig. 1. Schematic drawing of the experimental setup and a typical recording of a single C fiber firing. **a** Electrical stimuli were applied to the saphenous nerve of the rabbit hind limb in vivo. The nerve trunk was stimulated at S, and the antidromically propagating APs in a single C fiber were recorded at R. D and E indicate the drug pool and ground, respectively. **b** Stimulation protocol: trains of 5 superthreshold electrical stimuli with interstimulus intervals of 50 ms for a total of 1,000 pulses were applied to the nerve trunk. The interval between two trains was 1 s. Note that the interval of 50 ms was cut to show each pulse as clear as possible. **c** Representative recording of firing for a single C fiber evoked by the protocol in **b**. The lower three panels are the enlargements of the indicated regions in the upper panel. The artifact and the ISIs are illustrated in the third panel. Note that in the fourth panel, the AP was induced by the first electrical stimulation pulse (artifact$_1$).

interstimulus interval (i.e. the CV of posterior AP was slower than the preceding one), ΔISI was defined as positive, whereas 'faster' CV for posterior AP leading to shorter ISI was defined as negative ΔISI.

To determine whether conduction properties of C fibers changed across fibers, we analyzed the rCV according to the methods previously published [13]. In response to the quintuplet electrical pulses, 5 APs were initiated. For reasons of clarity, we named the first AP the leading AP and the other four APs the trailing APs (AP_{1-4}). To investigate the activity-dependent slowing of CV, we determined how the CV of the leading AP changed from the first to the last quintuplet pulse. To exclude the difference among C fibers, we normalized the data by calculating the rCV of the leading AP for each quintuplet pulse, which is denoted as the CV of the leading AP for a given quintuplet pulse divided by the CV of the leading AP for the first quintuplet pulse. We named this rCV for the leading AP with the symbol L. $L_n = (CV_{L,n}/CV_{L,1}) \times 100\%$, here $CV_{L,n}$ is the CV of the leading AP for the nth quintuplet pulse, $CV_{L,1}$ is the CV of the leading AP of the first quintuplet pulse. An $L < 100\%$ indicates a slowing of CV. To investigate whether the CV of each AP initiated by the quintuplet pulses changed during the whole stimulation, we computed the rCV of each AP by normalizing the data. For a given quintuplet pulse, the CVs of the trailing APs were divided by the CV of the

preceding AP, which is designated by the symbol T. $T_{1,n} = (CV_{1,n}/CV_{1,n-1}) \times 100\%$, where $T_{1,n}$ is the rCV of the first trailing AP for the nth quintuplet pulse and $CV_{1,n}$ is the CV of the first trailing AP of the nth quintuplet pulse. $CV_{1,n-1}$ is the CV of the first trailing AP of the $(n-1)$th quintuplet pulse. The other three Ts (i.e. T_2, T_3, and T_4) were assessed in an analogous manner. $T > 100\%$ indicates that the posterior trailing AP has a faster CV than the preceding one.

Chemicals

A blocker of hyperpolarization-activated cation current (I_h), ZD7288 (Tocris Cookson, UK), and an antagonist of 4-AP-sensitive potassium current ($I_{4\text{-AP}}$), (4-Aminopyridine, Sigma) were dissolved and diluted to the final concentrations with 0.9% saline and added into the drug administration pool, respectively (fig. 1a).

Statistical Analysis

All data are represented as means ± SEM. Data were analyzed using a paired or unpaired Student's t test as appropriate. $p < 0.05$ was considered statistically significant.

Results

Classification of C Fibers

In the present study, electrophysiological experiments were performed on 30 rabbits. The mean CV of C fibers was 0.91 ± 0.01 m/s (n = 40). A total of 200 quintuplets of superthreshold electrical pulses at interstimulus intervals of 50 ms were repetitively applied to the trunk of the saphenous nerve at a frequency of 1 Hz. Following the electrical stimulus, we measured the ISI between two successive APs evoked by the same interstimulus interval. Interestingly, ISI_{1-2} changed in a significantly different way compared to the interstimulus interval during the train stimulation, whereas the other ISIs (ISI_{2-3}, ISI_{3-4}, and ISI_{4-5}) were almost equal to this interval. According to the properties of ISI_{1-2} change during quintuplet stimuli at 50 ms interstimulus interval, a total of 40 C fibers tested in this experiment were classified into three types.

Thirteen units were classified as type 1 C fibers which were characterized by longer ISI_{1-2}. A typical ISI response pattern after the quintuplets of stimuli at interstimulus intervals of 50 ms is shown in figure 2a2. Repeated electrical stimuli induced a large change in ISI_{1-2} at the start which corresponded to $Max\Delta ISI_{1-2}$ (the maximal difference between ISI_{1-2} and the interstimulus interval), which decreased gradually and then stabilized at a new, longer ISI_{1-2} level. For this type of C fiber, ISI_{1-2} was always longer than the interstimulus interval during the whole trains applied to the nerve trunk. As shown in figure 2a3, ΔISI_{1-2} of type 1 was positive throughout the stimulation period. The response latency for the first AP and the second AP initiated by the 200 trains is indicated by the two solid lines (fig. 2a3).

Twelve units were classified as type 2 C fibers with wavelike ISI_{1-2} change. As shown in figure 2b2, repetitive stimulus applications evoked a pronounced change in ISI_{1-2}; ISI_{1-2} was initially longer than the interstimulus interval, then shorter, and finally longer in response to the 200 quintuplets. With successive repetitive stimuli, ISI_{1-2} also exhibited two time points where ISI_{1-2} was equivalent to the interstimulus interval. In contrast, the point where ISI_{1-2} decreased to the nadir was defined as $Max\Delta ISI_{1-2}$. During electrical stimulation with 200 quintuplets, ΔISI_{1-2} also showed a wavelike change, i.e. from positive to negative and then to positive again (fig. 2b3).

Fifteen units were classified as type 3 units, which were characterized by first longer and then shorter ISI_{1-2}. As shown in figure 2c2, ISI_{1-2} was longer than the interstimulus interval for a brief period at the beginning of repetitive stimulation. With further train stimuli, ISI_{1-2} decreased to a shorter value than the interstimulus interval and then to the nadir which corresponded to the $Max\Delta ISI_{1-2}$ of type 3. Following this point, ISI_{1-2} displayed a slight increase and then gradually stabilized at a new shorter level. Consistent with the ISI_{1-2} change, the ΔISI_{1-2} also exhibited negative values except for a short period of positive values at the beginning (fig. 2c3).

Relationship between ISI Changes and CV in the Three Types of C Fibers

To investigate the activity-dependent changes in the conduction properties of the three types of C fibers, we compared and analyzed the degree of the activity-dependent slowing (fig. 3). All three types of fibers exhibited activity-dependent slowing of CV where the velocity of the last leading AP was always less than the CV of the first leading AP. However, the conduction properties of the trailing APs were distinguished from the lead APs in these three types of C fibers. For type 1 fibers, the CV of the trailing APs was always slower than the leading AP (fig. 3a1, a2). For type 2 fibers, the CV of the trailing APs was initially slower, then faster, and then again slower than the CV of the leading AP at the end of the trial (fig. 3b1, b2). For type 3 fibers, the CV of the trailing APs was initially slower for a short time and then became faster than the CV of the leading AP for a long period (fig. 3c1, c2). However, there was no obvious difference among the CVs of the last trailing APs (i.e. trailing AP_2, trailing AP_3, and trailing AP_4). In addition, as shown in figure 2, the other three ISIs (ISI_{2-3}, ISI_{3-4}, and ISI_{4-5}) did not show any significant difference, but nearly matched the inter-

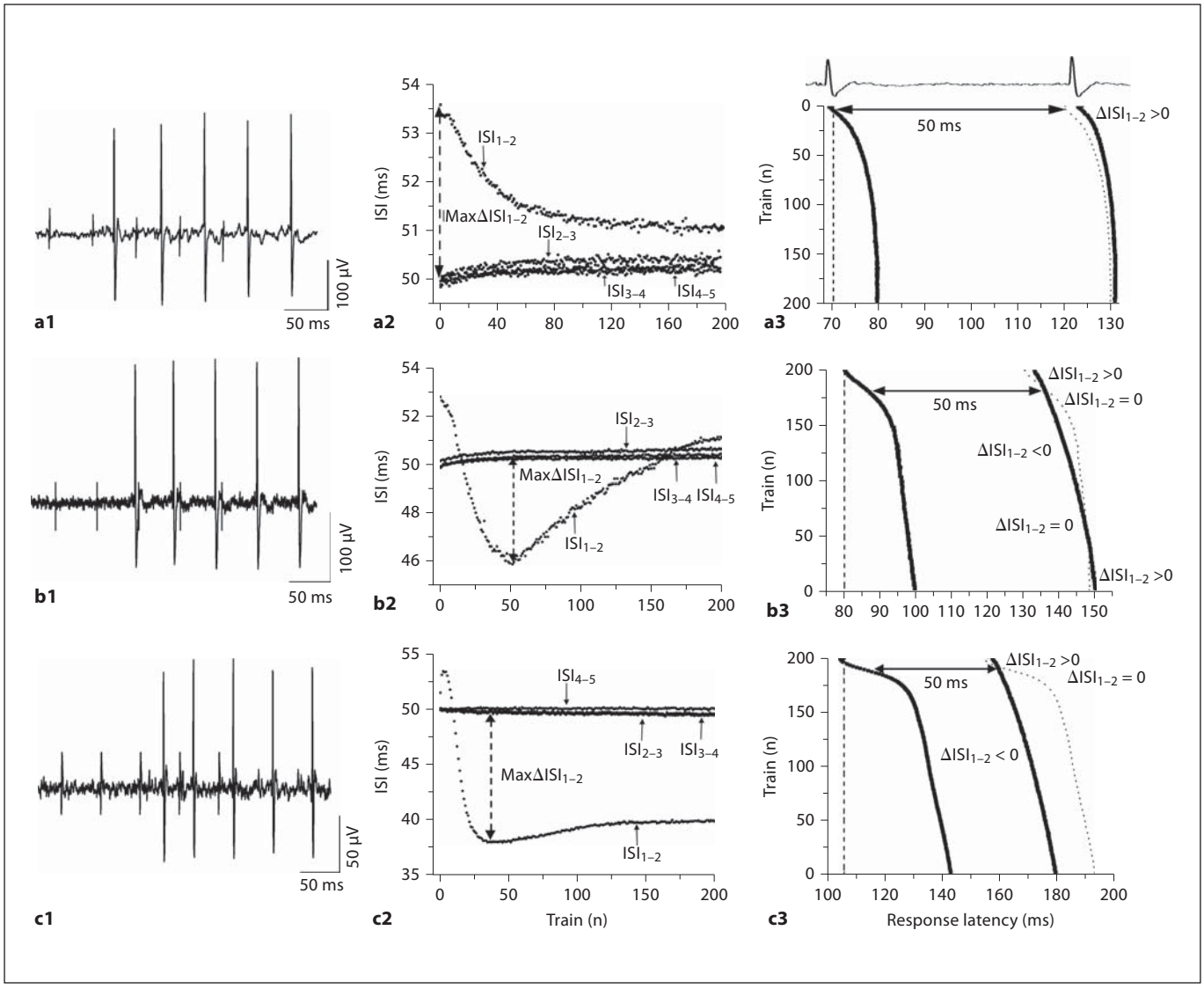

Fig. 2. Three types of ISI change and firing patterns induced by the quintuplet stimuli with the interval of 50 ms. **a1** A segment of original recording corresponding to $MaxΔISI_{1–2}$ from a type 1 C fiber (in **a2**), which shows a bigger $ISI_{1–2}$. **a2** The ISI series alteration in this type 1 C fiber during the 200 trains. Each point represents an ISI of two APs. Note that the ISI between the first and second AP ($ISI_{1–2}$) was always bigger than the interstimulus interval. **a3** Firing pattern of the initial two APs of the unit in **a2**. Top: trace of the initial two APs evoked by the electrical quintuplet pulse at 50 ms. For each of the successive traces, the response latencies of the initial two APs are tracked by solid lines from top to bottom. The difference between ISIs and interstimulus intervals is denoted as ΔISI. **b1** A segment of original recording corresponding to the point of $MaxΔISI_{1–2}$ from a type 2 C fiber (in **b2**), which shows a small $ISI_{1–2}$. **b2** The ISI series alteration of this type 2 C fiber during the 200 trains. Note that the $ISI_{1–2}$ exhibited a wavelike alteration compared to the interstimulus interval. **b3** Firing pattern of the initial two APs for the unit shown in **b2**. The difference between ISIs and interstimulus intervals is denoted as ΔISI. **c1** A segment of original recording corresponding to the point of $MaxΔISI_{1–2}$ from a type 3 C fiber (in **c2**), which shows a markedly small $ISI_{1–2}$. **c2** The ISI series alteration of this type 3 C fiber during the 200 trains. Note that the $ISI_{1–2}$ was bigger than the interstimulus interval at the beginning, then smaller than 50 ms and remained small thereafter. **c3** Firing pattern of the initial two APs of the unit shown in **c2**.

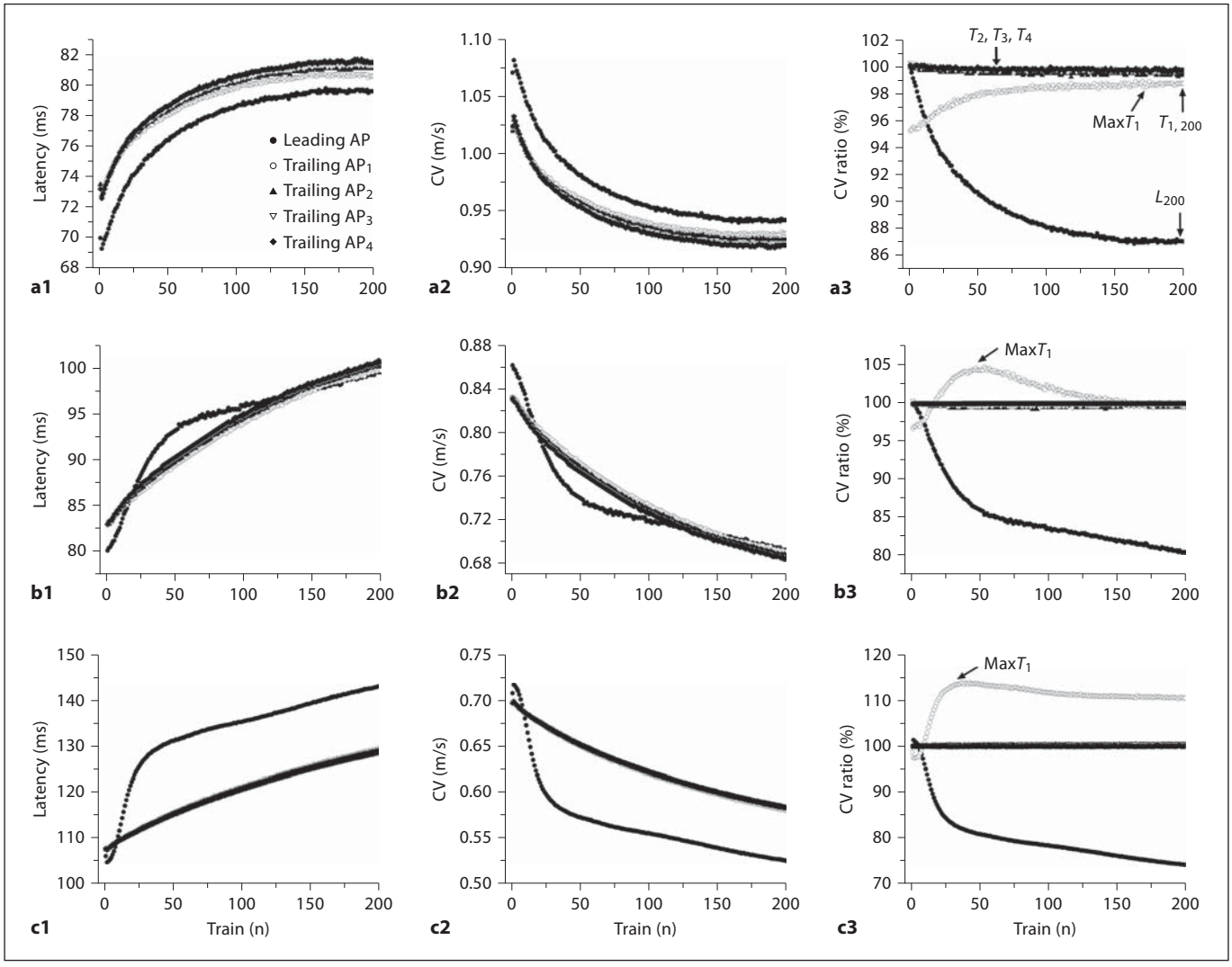

Fig. 3. Changes in CV during repeated electrical stimulation with an interval of 50 ms. **a1** The latency of the electrically evoked AP was used to measure how the CV varied with repeated stimulation. The AP latency of a type 1 C fiber in response to a quintuplet pulse of 200 trains. The first AP is denoted as the leading AP (filled circle), and the following 4 APs are denoted as trailing AP_1 (open circle), trailing AP_2 (filled triangle), trailing AP_3 (open triangle), and trailing AP_4 (filled diamond), respectively. **a2** The same data were converted to CV. **a3** The ratio of CV of the leading AP and trailing APs is normalized by the CV of the first leading AP. L is the CV of the leading AP divided by the CV of the first leading AP. T_1 is the CV of the first trailing AP (trailing AP_1) divided by the CV of the leading AP. The maximum of T_1 is denoted as MaxT_1. T_2 is the CV of the second trailing AP (trailing AP_2) divided by the CV of trailing AP_1. T_3 and T_4 were assessed in an analogous manner. **b1** The scatter plots of AP latency of a type 2 C fiber as a function of quintuplet pulse number. **b2** The same data were converted to CV. **b3** The rCV of the last leading AP (L_{200}) and the trailing APs (T_1, T_2, T_3, and T_4) was normalized by the CV of the first AP from the same data as **b1**. **c1** The plot of the AP latency of a type 1 C fiber as a function of quintuplet pulse number. **c2** CV was converted from the same data as **c1**. **c3** The ratio of CV of leading AP and trailing APs is normalized by the CV of the first leading AP.

stimulus interval. Therefore, in the following text, we focused on the analysis of changes in conduction properties of the first and second APs.

A scatter plot of the normalized CV of the leading AP (L, see details in Methods for normalization procedure) and the rCV of the trailing APs (T, see Methods) for each fiber is shown in figure 3a3, b3, and c3. Three parameters were used to characterize the activity-dependent changes in CV. As a measure of 'activity-dependent slowing/speeding', we computed L for the 200th train pulses (L_{200}).

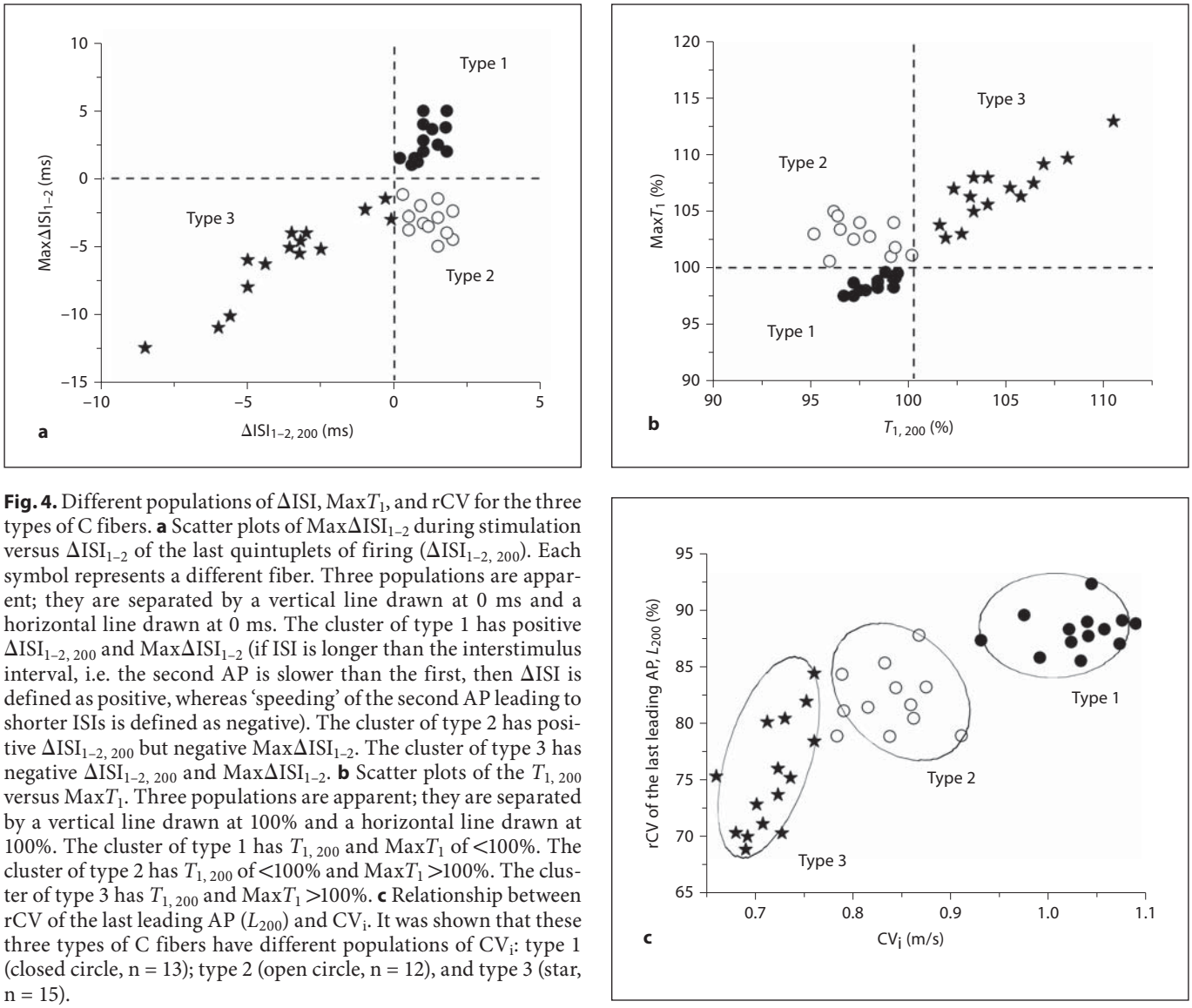

Fig. 4. Different populations of ΔISI, MaxT_1, and rCV for the three types of C fibers. **a** Scatter plots of MaxΔISI_{1-2} during stimulation versus ΔISI_{1-2} of the last quintuplets of firing ($\Delta ISI_{1-2,\ 200}$). Each symbol represents a different fiber. Three populations are apparent; they are separated by a vertical line drawn at 0 ms and a horizontal line drawn at 0 ms. The cluster of type 1 has positive $\Delta ISI_{1-2,\ 200}$ and MaxΔISI_{1-2} (if ISI is longer than the interstimulus interval, i.e. the second AP is slower than the first, then ΔISI is defined as positive, whereas 'speeding' of the second AP leading to shorter ISIs is defined as negative). The cluster of type 2 has positive $\Delta ISI_{1-2,\ 200}$ but negative MaxΔISI_{1-2}. The cluster of type 3 has negative $\Delta ISI_{1-2,\ 200}$ and MaxΔISI_{1-2}. **b** Scatter plots of the $T_{1,\ 200}$ versus MaxT_1. Three populations are apparent; they are separated by a vertical line drawn at 100% and a horizontal line drawn at 100%. The cluster of type 1 has $T_{1,\ 200}$ and MaxT_1 of <100%. The cluster of type 2 has $T_{1,\ 200}$ of <100% and MaxT_1 >100%. The cluster of type 3 has $T_{1,\ 200}$ and MaxT_1 >100%. **c** Relationship between rCV of the last leading AP (L_{200}) and CV_i. It was shown that these three types of C fibers have different populations of CV_i: type 1 (closed circle, n = 13); type 2 (open circle, n = 12), and type 3 (star, n = 15).

To quantify the possible supernormal conduction that might exist or develop during the trial, we measured the rCV of the last trailing AP_1 (i.e. $T_{1,\ 200}$) and the largest degree of slowing/speeding of the first trailing AP among all the 200 trains (Max T_1). As depicted in figure 3a3, both L_{200} and $T_{1,\ 200}$ of type 1 C fibers were <100% during the stimulation train, suggesting a CV slowing of the leading AP and the trailing AP_1. For type 2 C fibers, L_{200} was <100% but $T_{1,\ 200}$ experienced a wavelike change, showing less, more, and finally less than 100% under the whole stimulus (fig. 3b3). This is consistent with the CV change of the leading AP and the trailing AP_1 in figure 3b2. For type 3 C fibers, L_{200} exhibited <100% but $T_{1,\ 200}$ displayed >100% (fig. 3c3), which indicates that the CV slowing of the leading AP and CV speeding of the trailing AP_1 occur in response to the same stimulus.

To further assess whether these three types of C fibers have distinct conduction populations, we compared the changes in ISI_{1-2} and rCV of the leading AP and the trailing AP_1 among the three types of C fibers. To sum up, a scatter plot of MaxΔISI_{1-2} (i.e. the ΔISI_{1-2} with the largest absolute value compared to all ΔISI_{1-2} values) versus $\Delta ISI_{1-2,\ 200}$ (i.e. the ΔISI_{1-2} of the 200th quintuplet pulse) is shown in figure 4a. The type 1 fiber cluster has both positive MaxΔISI_{1-2} and positive $\Delta ISI_{1-2,\ 200}$. The type 2 fiber cluster showed a negative MaxΔISI_{1-2} and a positive

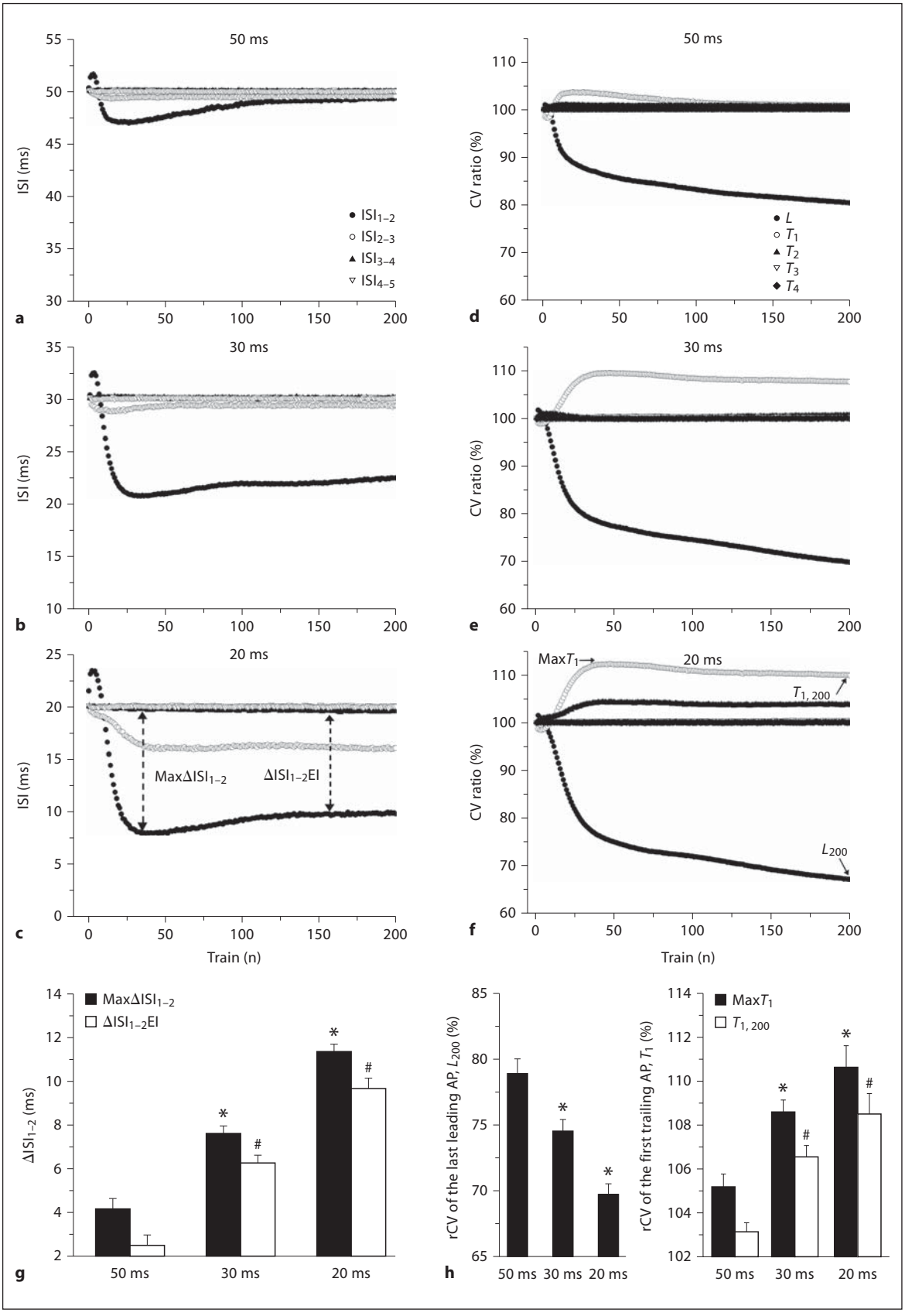

5

Neurosignals 2013;21:213–228
DOI: 10.1159/000337350

$\Delta ISI_{1-2,\,200}$, while the type 3 fiber cluster exhibited a negative $Max\Delta ISI_{1-2}$ and a negative $\Delta ISI_{1-2,\,200}$. Similarly, we found that there are three populations for the rCV of the trailing AP and the leading AP. The normalized data is shown in figure 4b, c. Both $T_{1,\,200}$ and $MaxT_1$ of type 1 fibers were <100%, suggesting the CV of the trailing AP_1 of type 1 fibers was always slower than that of the leading AP. For type 2 fibers, the rCV of the trailing AP_1 underwent an oscillatory change. $MaxT_1$ was >100%, but $T_{1,\,200}$ was <100%. In contrast, both $T_{1,\,200}$ and $MaxT_1$ of type 3 fibers were >100%. Taken together, these results suggest that the huge change in ISI_{1-2} might be associated with a CV slowing of the leading AP and a CV speeding/slowing of the trailing AP_1 for these three types of C fibers.

The Stimulus Frequency Dependence of ISI Change of Type 3 C Fibers

In figure 5, typical response patterns of type 3 C fibers after the 200 quintuplets of stimuli are compared at different interstimulus intervals (20, 30, and 50 ms). The scatter plot of ISIs showed that the ISI_{1-2} exhibited a pronounced increase compared to the other ISIs (ISI_{2-3}, ISI_{3-4}, and ISI_{4-5}) in response to the same stimulus (fig. 5a–c). To measure the change in the ISI_{1-2} at different stimulus frequencies, two parameters were designated, $Max\Delta ISI_{1-2}$ and $\Delta ISI_{1-2}EI$ (fig. 5c), where $Max\Delta ISI_{1-2}$ indicates the maximal difference between ISI_{1-2} and the interstimulus interval, and $\Delta ISI_{1-2}EI$ represents the interval when ISI_{1-2} reached an entrainment level [5]. As indicated in figure 5g, the average $Max\Delta ISI_{1-2}$ significantly increased from 4.15 ± 0.48 ms at an interstimulus interval of 50 ms to 7.57 ± 0.38 ms at an interval of 30 ms and 11.35 ± 0.34 ms at an interval of 20 ms ($p < 0.05$ compared to the interval of 50 ms, n = 10). The average $\Delta ISI_{1-2}EI$ also significantly increased from 2.48 ± 0.47 ms for an interstimulus interval of 50 ms to 6.24 ± 0.35 ms for an interval of 30 ms and 9.65 ± 0.48 ms for an interval of 20 ms ($p < 0.05$, n = 10). The histogram shows that both $Max\Delta ISI_{1-2}$ and $\Delta ISI_{1-2}EI$ increased in a stimulus frequency-dependent manner during the 200 trains.

To determine whether changes in the average CV of each AP is related to different interstimulus intervals for the 200 quintuplets, three parameters were determined: rCV of the leading AP (L), rCV of the trailing APs (T_1, T_2, T_3, and T_4), and maximal rCV of the trailing AP_1 for each train ($MaxT_1$). As indicated in figure 5d–f, an increase in stimulus frequency led to more activity-dependent slowing of the leading AP (L <100%), and the trailing AP displayed an enhanced CV speeding (T >100%). The histogram in figure 5h shows the normalized rCV of the last trailing AP_1 ($T_{1,\,200}$), $MaxT_1$, and rCV of the last leading AP (L_{200}). The average $MaxT_1$ increased from 105.14 ± 0.62% for 50 ms to 108.60 ± 0.61% for 30 ms and 110.65 ± 0.96% for 20 ms ($p < 0.05$ compared with the interstimulus interval of 50 ms, n = 10). The average $T_{1,\,200}$ was enhanced from 103.10 ± 0.44% for 50 ms to 106.55 ± 0.52% for 30 ms and 108.50 ± 0.95% for 20 ms. In comparison, the average L_{200} decreased from 78.90 ± 1.11% for 50 ms, 74.55 ± 0.85% for 30 ms, and 69.73 ± 0.76% for 20 ms. Taken together, these results suggest that the degree of change for ISI_{1-2} and activity-dependent conduction properties of type 3 C fibers might be associated with the stimulus frequency.

ISI Change Reduced by 4-AP

In our previous study, a fluctuation in ISIs was observed before conduction failure and 4-AP-sensitive potassium current ($I_{4\text{-AP}}$) was involved in the regulation of conduction failure patterns. To further investigate whether $I_{4\text{-AP}}$ mediates changes in ISIs and CV of each AP initiated by the electrical stimulus, we examined the effects of 4-AP on ISI changes and rCV in response to the quintuplet pulses for a total of 300 trains at the interstimulus interval of 20 ms in type 3 C fibers. As shown in figure 6a–c, ISI_{1-2} became obviously closer to the interstimulus interval with the increase in 4-AP concentration (20 and 40 μM). The average $Max\Delta ISI_{1-2}$ was significantly reduced from 12.75 ± 0.51 ms for control C fibers to 10.52

Fig. 5. Effects of different interstimulus intervals on ISI change and activity-dependent conduction properties of type 3 C fibers. **a–c** Typical ISI examples of a type 3 C fiber induced by stimulation at different frequencies (50, 30, and 20 ms from top to bottom). Note that the degree of ISI_{1-2} change was enhanced in a frequency-dependent manner. ISI_{2-3} was less than the interstimulus interval at 20 ms. The difference between ISI_{1-2} and interstimulus interval (ΔISI_{1-2}) increased with increased interstimulus frequency. ISI_{1-2} decreased asymptotically and approached the minimum 'entrainment' interval of the nerve fiber. **d–f** Activity-dependent CV changes at different frequencies (50, 30, and 20 ms from top to bottom). The rCV of the leading AP (L) and trailing AP_2 (T_2) was enhanced in a frequency-dependent manner. **g** Degree of ISI_{1-2} change was enhanced with an increase in stimulus frequency. Both $Max\Delta ISI_{1-2}$ and $\Delta ISI_{1-2}EI$ (the point where ΔISI_{1-2} reached the entrainment interval) significantly increased with the increase in stimulus frequency (n = 10). **h** Maximal rCV of the trailing AP_1 ($MaxT_1$) and the rCV of the last trailing AP_1 ($T_{1,\,200}$) were significantly enhanced with the increase in stimulus frequency. Activity-dependent slowing was enhanced with the increase in stimulus frequency. The rCV of the last leading AP (L_{200}) was significantly reduced with the increase of stimulus frequency (*, # $p < 0.05$, n = 10). All data are represented as means ± SEM.

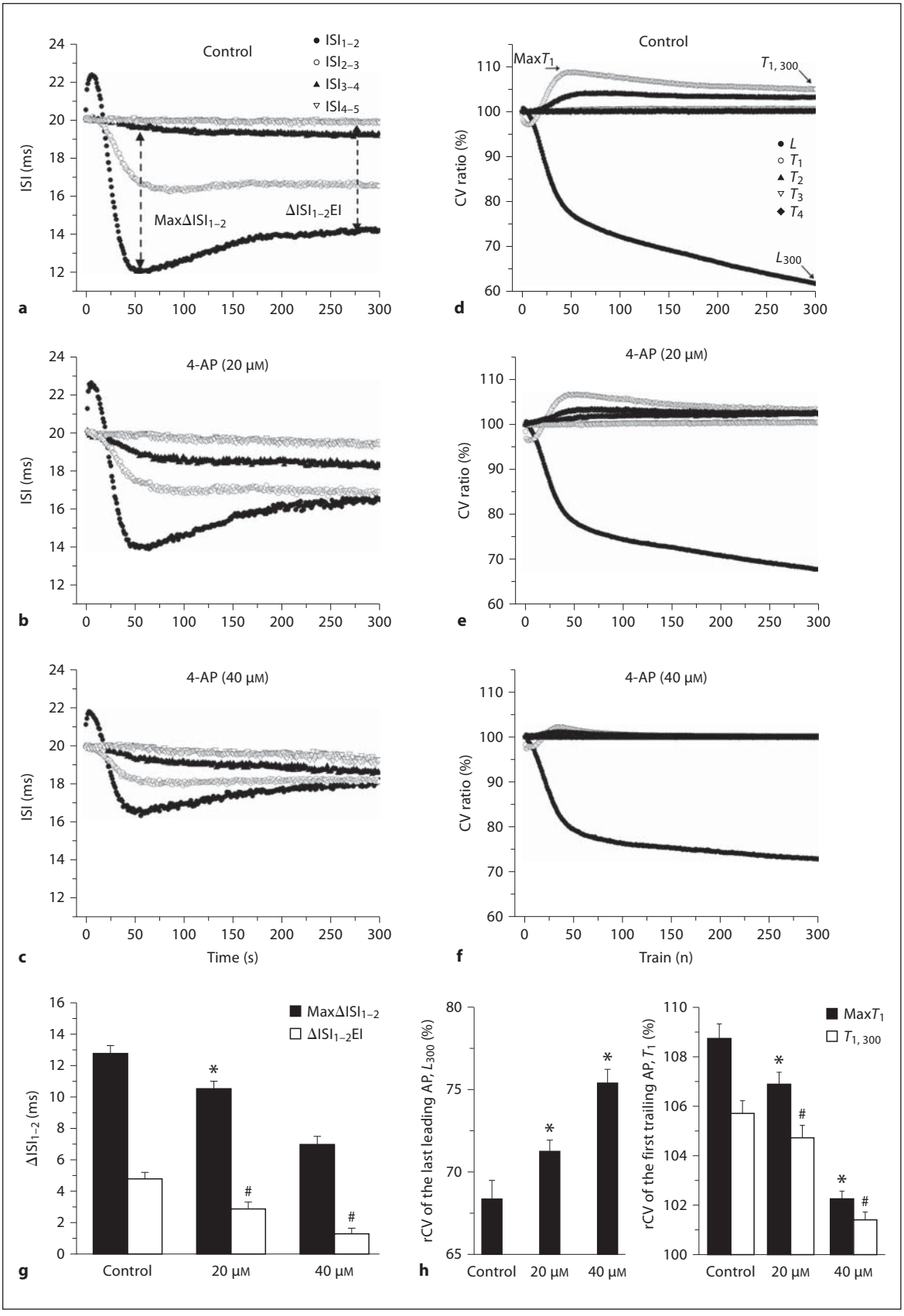
Control
ISI1–2
ISI2–3
ISI3–4
ISI4–5
ISI (ms)
MaxΔISI1–2
ΔISI1–2EI
a
Control
MaxT1
T1, 300
CV ratio (%)
L
T1
T2
T3
T4
L300
d
4-AP (20 μM)
b
e
4-AP (40 μM)
c
Time (s)
f
Train (n)
MaxΔISI1–2
ΔISI1–2EI
ΔISI1–2 (ms)
Control
20 μM
40 μM
g
rCV of the last leading AP, L300 (%)
h
MaxT1
T1, 300
rCV of the first trailing AP, T1 (%)

6

± 0.47 ms and 6.95 ± 0.53 ms for 20 and 40 μM 4-AP, respectively ($p < 0.05$ compared to control C fibers, n = 8). The average $\Delta ISI_{1-2}EI$ also significantly decreased from 4.76 ± 0.42 ms for control C fibers to 2.82 ± 0.48 ms for 20 μM 4-AP and 1.26 ± 0.37 ms for 40 μM 4-AP ($p < 0.05$, n = 8; fig. 6g). In addition, the effects of 4-AP on rCV of the leading AP and the trailing APs were tested in type 3 C fibers. As indicated in figure 6d–f, L_{300} was enhanced, whereas $T_{1,300}$ and MaxT_1 were reduced with increased 4-AP concentrations. In addition, the average value of L_{300} significantly increased from 68.37 ± 1.01% in control C fibers to 71.22 ± 0.83% in 20 μM 4-AP and 75.36 ± 0.70% in 40 μM 4-AP (fig. 6h, $p < 0.05$ compared to control C fibers, n = 8). The average MaxT_1 was 108.74 ± 0.60% for control C fibers, 106.91 ± 0.48% for 20 μM 4-AP, and 102.26 ± 0.31% for 40 μM 4-AP, respectively. In parallel, the average $T_{1,300}$ was reduced from 105.72 ± 0.50% for control C fibers to 104.73 ± 0.48% for 20 μM 4-AP and 101.41± 0.31% for 40 μM 4-AP ($p < 0.05$, n = 8). In the present experiments, 20 fibers were examined for drug application. Interestingly, although 5 fibers did not show decreased response to 4-AP, most of the fibers (15 of 20) exhibited the phenomenon mentioned above. These results indicate that 4-AP produces a reduction of ISI change with the increasing concentration for type 3 C fibers.

ISI Change Enhanced by ZD7288

As shown in figure 7a–c, following the electrical stimulation with the quintuplet pulses for a total of 300 trains at the interstimulus interval of 20 ms, local application of ZD7288 promoted changes in ISI with an increase in concentration (10–20 μM) for type 3 C fibers. More importantly, changes in MaxΔISI_{1-2} and $\Delta ISI_{1-2}EI$ were larger at higher concentrations of ZD7288. As indicated in figure 7g, the average MaxΔISI_{1-2} significantly increased from 12.01 ± 0.40 ms for control C fibers to 14.50 ± 0.58 ms for 10 μM ZD7288 and 17.05 ± 0.59 ms for 20 μM ZD7288 ($p < 0.05$ compared to control C fibers, n = 8). The average $\Delta ISI_{1-2}EI$ also significantly increased from 8.77 ± 0.70 ms for control C fibers to 9.51 ± 0.43 ms for 10 μM ZD7288 and 12.11 ± 0.56 ms for 20 μM ZD7288 ($p < 0.05$, n = 8). In contrast, L_{300} decreased during the stimulus train, showing activity-dependent CV slowing of the leading AP after the application of ZD7288. Additionally, both $T_{1,300}$ and MaxT_1 increased during the stimulus, exhibiting activity-dependent CV speeding of the trailing AP at the end of the trial in 10 and 20 μM ZD7288 (fig. 7d, e). Further quantitative analysis (fig. 7h) indicated that the average value of L_{300} was 70.61 ± 0.82% for control C fibers, 68.56 ± 0.86% for 10 μM ZD7288, and 66.18 ± 0.88% for 20 μM ZD7288. The average MaxT_1 was 108.07 ± 0.67% for control C fibers, 109.87 ± 0.77% for 10 μM ZD7288, and 111.68 ± 0.79% for 20 μM ZD7288. In parallel, the average $T_{1,300}$ was 106.24 ± 0.89% for control population, 107.94 ± 0.87% for 20 μM ZD7288 population, and 108.98 ± 1.01% for 20 μM ZD7288 population ($p < 0.05$, n = 8). Within the 22 fibers we examined, 12 C fibers exhibited the above-mentioned phenomenon, whereas 8 fibers exhibited no response, and 2 fibers a negative response (data not shown), suggesting that ZD7288 increases ISI change in a dose-dependent manner for type 3 C fibers.

Fig. 6. Effects of 4-AP on ISI change and activity-dependent conduction properties of type 3 C fibers in response to quintuplet pulse of 300 trains. **a–c** Representative ISI examples of a type 3 fiber induced by quintuplets of stimuli at an interstimulus interval of 20 ms were recorded before and 15 min after the application of 4-AP at different concentrations (control, 20, and 40 μM from top to bottom). The degree of ΔISI change for this type of C fiber decreased with the increase in the concentrations of 4-AP. Here, the ΔISI_{1-2} exhibited the most significant reduction. **d–f** Changes in rCV of trailing AP_1 (T_1) and the last leading AP (L_{300}) induced by different concentrations (control, 20, and 40 μM from top to bottom). The activity-dependent slowing of type 3 C fibers decreased with increasing concentrations of 4-AP. **g** Summarized data for dose-response curves for 4-AP (n = 8). Both the MaxΔISI_{1-2} and $\Delta ISI_{1-2}EI$ reduced with the increase in different concentrations of 4-AP. **h** Summarized data for the effects of 4-AP on the changes in the rCV of trailing AP_1 and L_{300}. The rCV of MaxT_1 and $T_{1,300}$ decreased with the increase in the concentrations of 4-AP, whereas the rCV of L_{300} increased with the enhancement of concentrations of 4-AP (*, # $p < 0.05$, n = 8). All data are represented as means ± SEM.

Discussion

New Types of C Fibers with Distinct Peripheral Processing

A previous study by Weidner et al. [5] showed that in humans, a train of impulses reached the knee at a lower rate than was the frequency of the stimulus, when the neural activity level is low. In contrast, high neural background activity increased the intra-train frequency from 50 Hz to the entrained maximum of 160 Hz in a train of four pulses. They concluded that at a given degree of neural accommodation, all afferent C-units exhibit a uniform pattern of aftereffects that were independent of fiber class [5]. In the present experiments, three types of C fibers were observed in recordings from the saphenous nerve of rabbits. Only the basic change features observed

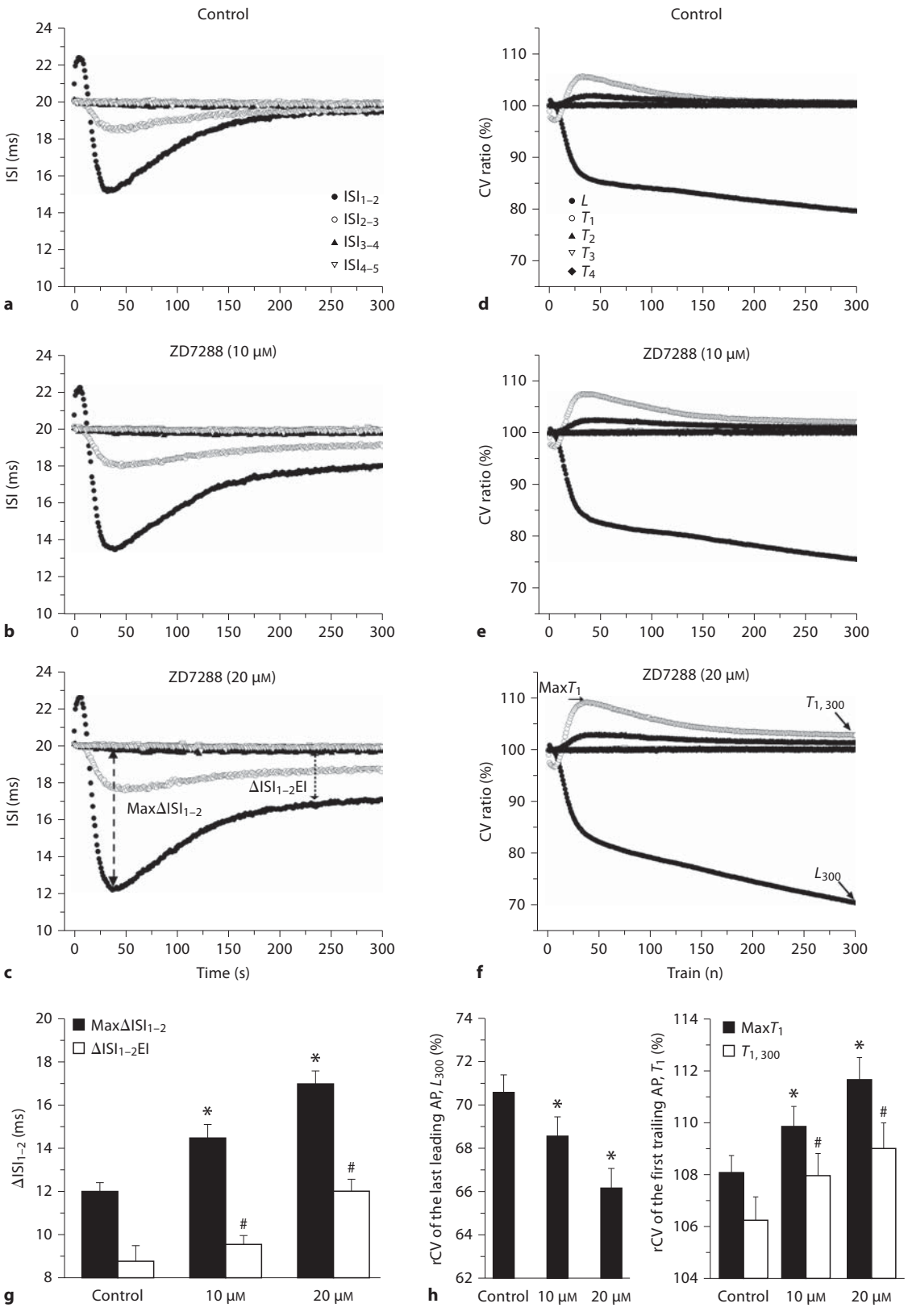
Control
ISI (ms)
ISI_{1-2}
ISI_{2-3}
ISI_{3-4}
ISI_{4-5}
a
ZD7288 (10 μM)
b
ZD7288 (20 μM)
$\Delta ISI_{1-2}EI$
$MaxΔISI_{1-2}$
Time (s)
c
CV ratio (%)
L
T_1
T_2
T_3
T_4
d
e
$MaxT_1$
$T_{1,300}$
L_{300}
Train (n)
f
$MaxΔISI_{1-2}$
$\Delta ISI_{1-2}EI$
ΔISI_{1-2} (ms)
Control
10 μM
20 μM
g
rCV of the last leading AP, L_{300} (%)
h
rCV of the first trailing AP, T_1 (%)

7

for type 3 C fibers (fig. 2c2, c3) resemble the results in Weidner et al.'s report. That is, in type 3 cells ISI_{1-2} was larger initially and then decreased to a stable interval compared to the interstimulus interval. In parallel, the ΔISI_{1-2} also changed from a short, positive period to a negative value in 'entrainment'. However, the characteristics of ISI_{1-2} for type 1 and type 2 C fibers observed in the present study were different from those of type 3, suggesting that all afferent C fibers do not exhibit a uniform pattern of aftereffects, which may depend on different intrinsic properties of C fibers.

Recently, Shim et al. [13] reported that two populations of C fibers showed different activity-dependent slowing of CV. One C fiber group exhibited a large amount of slowing of CVs and was presumed to consist of nociceptors. The other group exhibited a smaller degree of activity-dependent slowing and was presumed to consist of non-nociceptors, such as cold fibers, mechanoreceptors, and sympathetics. In the present study, these basic features of rCV may correspond to type 1 and type 3 C fibers (fig. 3a3, c3). However, the wavelike change in T_1 from type 2 C fibers (fig. 3b3) has not been reported; this may represent a new type of C fiber.

Possible Reason for the Marked Changes in ISI Restricted to the ISI_{1-2} of Train Series

It is well known that the degree of CV slowing is closely related to the stimulus frequency and the interval between the condition impulses and test impulses [10, 14]. In addition, when the stimulus frequency is constant, the degree of change for aftereffects in the CV mainly depends on the interval between conditioning and test impulses. In the present study, C fibers were stimulated with trains of 5 pulses at a constant frequency (20 Hz) for 200 s. It was observed that the distinct changes in the ISI series were restricted to ISI_{1-2} and not present in the other three ISIs (ISI_{2-3}, ISI_{3-4}, and ISI_{4-5}; fig. 2). We hypothesized that in an AP series with regular train patterns, the interval between conditioning and test impulses becomes the main factor for determining the degree of aftereffect on ISI. We believe that two kinds of aftereffects may be involved in regulating the ISI series. One is a 'longer-interval (>800 ms) aftereffect' from the preexisting trains, the other is a 'shorter-interval (about 50 ms) aftereffect' which occurred mainly within the intra-burst of the trains. In the train-firing series, the first AP of the burst (the leading AP) might mainly be subjected to the longer-interval aftereffect which induces a relatively smaller CV slowing. In contrast, the second AP of the burst (the trailing AP_1) might be influenced by the shorter-interval aftereffect as well as the longer aftereffect. This shorter-interval aftereffect may have a more prominent effect on activity-dependent slowing; thus, the combined action of these two kinds of aftereffects could result in a larger CV slowing. Taken together, ISI_{1-2} of the burst in the train series exhibits a greater change in interval, while the other three ISIs (ISI_{2-3}, ISI_{3-4}, and ISI_{4-5}) experience less change because of their approximately equivalent aftereffects. Consistent with this result, Weidner et al. [5] reported that the response of a C fiber to quadruplets of stimuli at an interstimulus interval of 20 ms showed a larger change restricted to the ISI_{1-2}. Furthermore, the above-mentioned phenomenon could be partially explained by the 'passive time constant' theory. An afterpotential is corresponding to $(Q_{Na} - Q_K)/C$, where Q_{Na} and Q_K is the quantity of Na^+ and K^+ ions flowing into the axon, and C is the capacitance of the membrane. When $Q_{Na} = Q_K$, all afterpotentials and post-spike velocity changes are absent due to the 'passive time constant' mechanism [9]. This may account for the lack of changes in the other three ISIs. Obviously, different stimuli protocols could alter the time order of aftereffect on the ISI series by changing the distribution of activity-dependent effects.

Biophysical Properties Underlying Type-Specific ISI Change Patterns

Specific patterns of activity-dependent changes in ISIs likely result from differences in the activity of many processes, including an activity-dependent time course of

Fig. 7. Effects of ZD7288 on ISI change and activity-dependent conduction properties of type 3 C fibers in response to a quintuplet pulse of 300 trains. **a–c** Typical ISI examples of a type 3 fiber induced by the quintuplets of stimuli at an interstimulus interval of 20 ms were recorded before and after the application of ZD7288 with different concentrations (control, 10, and 20 μM from top to bottom). The degree of ΔISI changes for this type of C fiber enhanced with the increase in the concentration of ZD7288, especially for ΔISI_{1-2}. **d–f** Changes in rCV of the trailing AP_1 (T_1) and the leading AP in response to increasing trains with different concentrations (control, 10, and 20 μM from top to bottom). The activity-dependent slowing of type 3 C fibers enhanced with the increase in the concentration of ZD7288. **g** Summarized data for dose-response curves for ZD7288 (n = 8). Both the $Max\Delta ISI_{1-2}$ and $\Delta ISI_{1-2}EI$ increased with increasing concentrations of ZD7288. **h** Summarized data for the effects of ZD7288 on changes in rCV of the trailing AP_1 and L_{300}. The rCV of $MaxT_1$ and $T_{1,300}$ increased with rising concentrations of ZD7288, while the rCV of L_{300} decreased with the enhancement of concentrations of ZD7288 (*, # $p < 0.05$, n = 8). All data are represented as means ± SEM.

post-excitatory effects. We found that type 1 C fibers did not exhibit activity-dependent CV speeding as a sign of a supernormal period, which was apparent with the stimulus parameters used for the other two types of fibers. Because Weidner et al. [5] and Bostock et al. [9] found that some mechano-responsive (CMR) fibers have long-lasting time-dependent subnormality but not supernormality, we hypothesized that type 1 C fibers may be a kind of CMR fiber. In addition, we found that type 1 fibers showed less CV slowing than the other two types of C fibers. In the present study, type 2 C fibers exhibited both activity-dependent CV speeding and CV slowing, showing that ISI_{1-2} fluctuated around the stimulus interval. On the other hand, we found that type 2 fibers reached apparent CV slowing within 50 pulses after the onset, but the latency reversed partially during the remainder of the stimulation train (fig. 3b1, b3). Such a pattern of slowing is a characteristic of sympathetic efferents [18]. In addition, studies showed that recovery cycles of sympathetic units include both supernormal and subnormal velocities [9, 18]. Accordingly, we propose type 2 C fibers to be 'sympathetic-like', although additional study is needed. Furthermore, we found that ISI_{1-2} of type 3 C fibers increased for a shorter period initially, but then decreased at high levels of activity-dependent accommodation, which asymptotically approached the minimum 'entrainment' interval of the nerve fibers. This result is consistent with the pattern of ISI changes for CMR and heat-responsive (CMH) efferents in humans [5]. Accordingly, we propose that type 3 C fibers are CMH fibers. However, these suppositions may be open to different interpretations since other types of fibers, such as mechanically insensitive afferents and cold afferents, have not been examined in our studies.

Ionic Mechanisms Underlying ISI Changes

In the present study, we observed that application of 4-AP resulted in a decrease of ISI change (fig. 6). In some cases, at a higher concentration of 4-AP, all four ΔISIs were reduced approximately to zero. It is well known that Na^+-K^+ pump activity can be markedly blocked by 4-AP in concentration- and voltage-dependent manners [19]. In addition, several studies have shown an inhibitory effect of 4-AP on voltage-gated tetrodotoxin-sensitive sodium currents [20]. Massive influx of sodium during repetitive spiking can activate the pump which in turn causes prolonged after-hyperpolarization. On the other hand, 4-AP can block K^+ channels and reduce the K^+ conductance [21]. In addition, 4-AP strongly facilitates the influx of calcium in unmyelinated axons [22]. The factors listed above can inhibit the pump activity directly or indirectly, reducing membrane hyperpolarization level, which then results in a decreased CV slowing. Therefore, the decrease of CV slowing may be the reason for the decrease in positive ΔISI at the initial times. Moreover, many studies have demonstrated that the presence of an activity-induced slowing of conduction is the prerequisite for CV speeding in the supernormal period, and its degree determines the amount of speeding [5, 9, 12]. Consequently, the decrease of CV slowing induced a subsequent decrease in negative ΔISI after the application of 4-AP.

In contrast, on the main axons of C fibers, blockade of I_h by its antagonist ZD7288 enhanced ISI change. A previous report indicated that ZD7288 enhanced the activity-dependent slowing of conduction seen in C fiber compound APs recorded from isolated rat vagus nerves and also augmented the post-tetanic hyperpolarization following trains of APs in unmyelinated and myelinated axons [23]. Consistent with this result, Soleng et al. [24] found that an activity-induced hyperpolarization could be partly countered by I_h in hippocampal Schaffer collaterals and concluded that I_h may play a role in maintaining excitability and reliable conduction during AP activity. In addition, hyperpolarization of the membrane produces different activation/inactivation states of other voltage-gated ion channels. For example, ZD7288 perfusion produces an after-hyperpolarization that accelerates the removal of inactivation from sodium channels, which allows more sodium ions to flow into the axon during repetitive spiking. The massive influx of sodium ions then activates the pump which in turn causes prolonged after-hyperpolarization. Taken together, these results suggest that the application of ZD7288 could result in further hyperpolarization of the axon, which leads to an increase of CV slowing and increase of ΔISI at early time. In support of this idea, we also found the subsequent increase of negative ΔISI and entrainment interval after ZD7288 perfusion.

Functional Implications of Peripheral Signal Processing

In previous studies, researchers paid close attention to the role of nociceptors and sensory neurons in pain generation [25, 26]. For example, some C fiber receptor terminals exhibit adaptation in response to a constant superthreshold stimulus. This kind of adaptation plays an important role in temporal summation mechanisms of tonic cutaneous mechanical pain [27]. Another example is neuropathic pain, which is characterized by spontaneous pain and tactile allodynia, i.e. pain evoked by normally innocu-

ous mechanical stimuli. Ectopic discharges developed in neurons of the dorsal root ganglion after peripheral nerve injury or inflammation are considered as painful signals for the generation and maintenance of neuropathic pain [17–29]. However, based on the results of the present study, the temporal pattern of APs may, in part, be due to the changes in ISIs during the conduction of spikes in C fibers. In other words, the temporal pattern of the response to natural stimuli may be modulated peripherally.

The fact that the axon modifies the coding of AP trains may explain the changes in the responses associated with various pathologies. For example, activation of axonal 5-HT (3) receptors, an important inflammatory mediator, not only enhanced membrane excitability, but also modulated AP trains in nociceptive C fibers at high impulse rates [6]. Uninjured C fibers in the L4 spinal nerve exhibited increased activity-dependent slowing following L5 spinal nerve injury in rats. The enhanced slowing can result in an increase in instantaneous frequency of a burst discharge when it reaches the spinal cord [30]. Altered properties of axonal excitability in amyotrophic lateral sclerosis induce a longer and irregular interval ectopic impulse, which causes fasciculations [31]. Regular high-frequency bursts occur when axons are strongly hyperpolarized by increased Na^+ pumping. The regular high-frequency bursts are the reasons for the sensation of 'pins and needles' following a prolonged period of limb ischemia [32]. Demyelinating diseases, such as multiple sclerosis, are associated with both negative and positive symptoms. Positive symptoms are caused by regular ectopic discharges from demyelinated axons perceived as paresthesia [33]. Based on these data, we hypothesize that in some pathological conditions the adaptation properties may be perturbed by altering both numbers and patterns of firing series, ultimately influencing perception or movement. In the present study, we found the peripheral process of firing series can change temporal structure in different types of C fibers, which strongly suggests that the function of information processing could also occur in the propagation course along the main axon of C fibers.

Acknowledgments

We thank Prof. Grant D. Nicol (Indiana University School of Medicine, Indianapolis, Ind., USA) for his serious reading and modification of the manuscript. This work was supported in part by the National Scientific Foundation of China Key Grant (30530260), National Scientific Foundation of China (31100759), and Scientific Foundation of Chongqing (CSTC2011BB5039).

References

1 Bishop GH: My life among the axons. Annu Rev Physiol 1965;27:1–18.
2 Mackenzie PJ, Umemiya M, Murphy TH: Ca2+ imaging of CNS axons in culture indicates reliable coupling between single action potentials and distal functional release sites. Neuron 1996;16:783–795.
3 Debanne D, Campanac E, Bialowas A, Carlier E, Alcaraz G: Axon physiology. Physiol Rev 2011;91:555–602.
4 Bucher D, Goaillard JM: Beyond faithful conduction: short-term dynamics, neuromodulation and long-term regulation of spike propagation in the axon. Prog Neurobiol 2011;94:307–346.
5 Weidner C, Schmelz M, Schmidt R, Hammarberg B, Orstavik K, Hilliges M, Torebjörk HE, Handwerker HO: Neural signal processing: the underestimated contribution of peripheral human C-fibers. J Neurosci 2002;22:6704–6712.
6 Lang PM, Moalem-Taylor G, Tracey DJ, Bostock H, Grafe P: Activity-dependent modulation of axonal excitability in unmyelinated peripheral rat nerve fibers by the 5-HT (3) serotonin receptor. J Neurophysiol 2006;96:2963–2971.
7 George A, Serra J, Navarro X, Bostock H: Velocity recovery cycles of single C fibres innervating rat skin. J Physiol 2007;578:213–232.
8 Stys PK, Ashby P: An automated technique for measuring the recovery cycle of human nerves. Muscle Nerve 1990;13:750–758.
9 Bostock H, Campero M, Serra J, Ochoa J: Velocity recovery cycles of C fibres innervating human skin. J Physiol 2003;553:649–663.
10 Gee MD, Lynn B, Cotsell B: Activity-dependent slowing of conduction velocity provides a method for identifying different functional classes of C-fibre in the rat saphenous nerve. Neuroscience 1996;73:667–675.
11 Shin HC, Raymond SA: Excitability changes in C fibers of rat sciatic nerve following impulse activity. Neurosci Lett 1991;129:242–246.
12 Weidner C, Schmidt R, Schmelz M, Hilliges M, Handwerker HO, Torebjörk HE: Time course of post-excitatory effects separates afferent human C fibre classes. J Physiol 2000;527:185–191.
13 Shim B, Ringkamp M, Lambrinos GL, Hartke TV, Griffin JW, Meyer RA: Activity-dependent slowing of conduction velocity in uninjured L4 C fibers increases after an L5 spinal nerve injury in the rat. Pain 2007;128:40–51.
14 Chi SM, Hu SJ, Liu K, Ren W: Variability of conduction velocity in unmyelinated nerve fibers after excitation (in Chinese). J Fourth Milit Med Univ 1997;18:119–122.
15 Zhu ZR, Tang XW, Wang WT, Ren W, Xing JL, Zhang JR, Duan JH, Wang YY, Jiao X, Hu SJ: Conduction failures in rabbit saphenous nerve unmyelinated fibers. Neurosignals 2009;17:181–195.
16 Chen X, Levine JD: Hyper-responsivity in a subset of C-fiber nociceptors in a model of painful diabetic neuropathy in the rat. Neuroscience 2001;102:185–192.
17 Hu SJ, Zhu J: Sympathetic facilitation of sustained discharges of polymodal nociceptors. Pain 1989;38:85–90.
18 Campero M, Serra J, Bostock H, Ochoa JL: Partial reversal of conduction slowing during repetitive stimulation of single sympathetic efferents in human skin. Acta Physiol Scand 2004;182:305–311.

19 Wang XQ, Xiao AY, Yang A, LaRose L, Wei L, Yu SP: Block of Na+, K+-ATPase and induction of hybrid death by 4-aminopyridine in cultured cortical neurons. J Pharmacol Exp Ther 2003;305:502–506.

20 Lu BX, Liu LY, Liao L, Zhang ZH, Mei YA: Inhibition of Na+ channel currents in rat myoblasts by 4-aminopyridine. Toxicol Appl Pharmacol 2005;207:275–282.

21 Del Negro CA, Chandler SH: Physiological and theoretical analysis of K+ currents controlling discharge in neonatal rat mesencephalic trigeminal neurons. J Neurophysiol 1997;77:537–553.

22 Bielefeldt K, Jackson MB: A calcium-activated potassium channel causes frequency-dependent action-potential failures in a mammalian nerve terminal. J Neurophysiol 1993; 70:284–298.

23 Takigawa T, Alzheimer C, Quasthoff S, Grafe P: A specific blocker reveals the presence and function of the hyperpolarization-activated cation current IH in peripheral mammalian nerve fibres. Neuroscience 1998;82:631–634.

24 Soleng AF, Chiu K, Raastad M: Unmyelinated axons in the rat hippocampus hyperpolarize and activate an H current when spike frequency exceeds 1Hz. J Physiol 2003;552: 459–470.

25 Torebjörk HE, Schady W, Ochoa JL: A new method for demonstration of central effects of analgesic agents in man. J Neurol Neurosurg Psychiatry 1984;47:862–869.

26 Jørum E, Lundberg LE, Torebjörk HE: Peripheral projections of nociceptive unmyelinated axons in the human peroneal nerve. J Physiol 1989;416:291–301.

27 Andrew D, Greenspan JD: Peripheral coding of tonic mechanical cutaneous pain: comparison of nociceptor activity in rat and human psychophysics. J Neurophysiol 1999;82: 2641–2648.

28 Liu CN, Wall PD, Ben-Dor E, Michaelis M, Amir R, Devor M: Tactile allodynia in the absence of C-fiber activation: altered firing properties of DRG neurons following spinal nerve injury. Pain 2000;85:503–521.

29 Hu SJ, Xing JL: An experimental model for chronic compression of dorsal root ganglion produced by intervertebral foramen stenosis in the rat. Pain 1998;77:15–23.

30 Serra J, Campero M, Ochoa J, Bostock H: Activity-dependent slowing of conduction differentiates functional subtypes of C fibres innervating human skin. J Physiol 1999;515: 799–811.

31 Layzer RB: The origin of muscle fasciculations and cramps. Muscle Nerve 1994;17: 1243–1249.

32 Baker MD: Axonal flip-flops and oscillators. Trends Neurosci 2000;23:514–519.

33 Barrett EF, Barrett JN: Intracellular recording from vertebrate myelinated axons: mechanism of the depolarizing afterpotential. J Physiol 1982;323:117–144.